International Journal of Applied Mathematics

Volume 37 No. 3 2024, 311–332
ISSN: 1311-1728 (printed version); ISSN: 1314-8060 (on-line version)
doi: http://dx.doi.org/10.12732/ijam.v37i3.3

A NOVEL APPROACH FOR SOME FIXED POINT RESULTS IN COMPLETE G-METRIC SPACE BY USING ASYMPTOTICALLY REGULAR MAPPING IN DIGITAL IMAGE COMPRESSION AND DECOMPRESSION APPLICATIONS

R. Anna Thirumalai [1], **S. Thalapathiraj** [2,§]

[1,2] Department of Mathematics

Faculty of Engineering and Technology

SRM Institute of Science and Technology

Vadapalani Campus

No.1 Jawaharlal Nehru Salai, Vadapalani

Chennai - 26, Tamil Nadu, INDIA

[1] e-mail: ar1546@srmist.edu.in

[2,§] e-mail: thalapas@srmist.edu.in

Abstract

In this paper, we extend some unique fixed point theorem results on a complete symmetric G-metric space by using asymptotically regular mappings with a new approach. Moreover, the new structure of extended G-contractive mapping on suitable spaces is used to create images with reduced size in this paper. A digital image is a representation of two-dimensional pixels arrays. A mild but typical system of extended G-contractive mapping on the Euclidean plane, known as the digital plane, is implemented for image processing to produce images with compressed dimensions that take up less storage space and can be transmitted efficiently. The size of the initial picture matrix has

Received: October 10, 2023

been reduced dramatically on decreasing the order of sub-matrices, resulting in images of reduced size with little loss in image quality. When images are enlarge and appeared in a short screen, the variations between the original and reduced image are not as noticeable (mobile, tablets, etc.)

MSC 2020: 47H10, 54H25

Key Words and Phrases: fixed point, asymptotically regular mapping, G-cauchy sequence, G-metric space, matrix distance, digital image, data compression

1. **Introduction**

Fixed point theory in metric space is a major research area in both applied and pure mathematics, and its applications are useful in various fields throughout science and engineering. This theory is based on the Banach contraction principle in metric spaces. The most essential mathematical test for various problem solutions is the Banach fixed point theorem. In 1922, [1] Banach presented the Banach Contraction Mapping Principle. Later, many authors found various types of metric spaces such as 2-metric space, b-metric space, D-metric space, G-metric space, S-metric space, cone metric space, and complex-valued metric space are some generalisations of a metric space. In 1963, [2] Gahler first introduced the concept of a 2-metric space. The only space, that is not topologically comparable to an ordinary metric, is a 2-metric space. But the results produced in metric spaces and 2-metric spaces could not be easily related to one another. As a result, in 1984, [3] Dhage introduced the idea of a D-metric spaces.

After that, [4] in 2003, Mustafa and Sims showed that the majority of topological characteristics of D-metric spaces were incorrect. Then, G-metric space was first established by Mustafa and Sims [5] and several fixed point theorems on G-metric spaces were obtained. The majority of the fixed point theorems on G-metric spaces that have been discovered, as per [17] can be directly deduced from the fixed point theorems on metric or quasi-metric spaces. The concept of Asymptotically regular at a point in space [8] was initially introduced by Browder and Petryshyn in 1966. Some fixed point results in complete symmetric G-metric space is shown in this paper using asymptotically regular mapping with a new contractive condition. The idea is useful in determining the existence and uniqueness of fixed point theory, [22, 24, 23] and it is at the core of a wide set of image processing tools.

The digital fundamental group [15] of a discrete object is then introduced by Han in 2006. In 1979, Rosenfeld founded field of digital topology, [19] which has had a significant impact on many areas of applications including image processing, pattern recognition, and the development of the concept of digital continuity for 2D and 3D digital images [30, 31, 32]. A complete digital metric

space [13] has been developed by Bosilj et al. in 2018. In 1994, [7] Boxer analyzed a variety of digital continuous functions and produced digital analogs of several topological ideas. The study of the topological characteristics of image arrays is known as digital topology. The outcomes offer a solid mathematical foundation for operations on images, including picture thinning, contour filling and object counting. The study of the features of 2D and 3D digital images is known as digital topology, a developing field in general topology and functional analysis. In 2012, [9] Karaca and Ege provided several results and defined characteristics about the digital homology groups of 2D [12] digital images. In 2015, [10] Ege and Karaca proved the Lefschetz fixed point theorem for digital images and demonstrated that sphere-like digital images have the fixed point property. Digital imaging systems have expanded in recent years due to developments in digital camera technology.

The need for storage space is growing as the demand for large image files grows. As an application of extended G-contractive mappings, the authors propose an extended G-contraction approach for reducing the size of image files. Image resizing (reduction) is accomplished by reducing overall number of pixels. The goal is to get an image proportionately smaller than the input image, which has a size of $m \times n$. The original digital image is processed to reduce its size, and the image that is finally presented on the screen is not precisely the same as the original because distortions are introduced in exchange for the size reduction, but it will be a good representation of the original image. The quality of the processed image is certified not only by subjective methods that include humans evaluating the image but also by objective image quality measurements such as PSNR [26, 11], which mathematically measures the image quality.

2. **Basic concepts**

DEFINITION 2.1. Let X be a non empty set, and let $G : X \times X \times X \to R^+$ be a function satisfying the following properties:

(1) $G(x, y, z) = 0$ if $x = y = z$,
(2) $G(x, x, y) > 0$; for all $x, y \in X$ with $x \neq y$,
(3) $G(x, x, y) \leq G(x, y, z)$ for all $x, y, z \in X$ with $y \neq z$,
(4) $G(x, y, z) = G(x, z, y) = G(y, z, x) = ...$
(symmetry in all three variables),
(5) $G(x, y, z) \leq G(x, a, a) + G(a, y, z)$ for all $x, y, z, a \in X$
(rectangle inequality).

Then the function G is called a generalized metric or more specially, a G-metric on X, and (X, G) is called a G-metric space.

DEFINITION 2.2. Let (X, G) be a G-metric space.

(1) The sequence $\{x_n\}$ G-convergent to $x \in X$ if and only if $\lim_{n,m\to\infty} G(x, x_n, x_m) = 0$.
(2) The sequence $\{x_n\}$ G-Cauchy if and only if $\lim_{n,m,l\to\infty} G(x_n, x_m, x_l) = 0$.
(3) (X, G) is G-complete if and only if every G-Cauchy sequence in X is G-convergent.

DEFINITION 2.3. A mapping $T : X \to X$ of a symmetric G-metric space (X, G) into itself is said to be asymptotically regular mapping at a point $x \in X$, if

$$\lim_{n\to\infty} G(T^{n+1}x, T^n x, T^n x) = 0, \tag{1}$$

$$\lim_{n\to\infty} G(T^n x, T^{n+1}x, T^{n+1}x) = 0, \tag{2}$$

where $T^n x$ is n^{th} iterate of T at $x \in X$".

DEFINITION 2.4. The matrix A is given by Frobenius norm as:

$$\rho_F = \sqrt{\sum_{i=1}^{m}\sum_{j=1}^{n}(a_{ij})^2} = \sqrt{trace(AA')}. \tag{3}$$

DEFINITION 2.5. The difference between two images is calculated using the peak signal-to-noise ratio (PSNR), which is defined as

$$PSNR = 10log_{10}\left\{\frac{b \times b}{rms}\right\}. \tag{4}$$

For illustration in this study, an 8-bit test image is chosen, therefore $b = 255$.

3. The main results

THEOREM 3.1. *In a complete symmetric G-metric space (X, G), a self mapping $T : X \to X$ has a unique fixed point if there exists an asymptotically regular mapping with for all $x, y, z \in X$, and*

$$\begin{aligned} G(Tx, Ty, Tz) \leq\ & \alpha G(x, y, z) \\ & + \beta[G(Tx, x, Tx) + G(Ty, y, Ty) + G(Tz, z, Tz)] \\ & + \gamma[G(Tx, y, Tx) + G(Tx, z, Tx) + G(Ty, x, Ty) \\ & + G(Ty, z, Ty) + G(Tz, x, Tz) + G(Tz, y, Tz)] \\ & + \delta[G(Tx, x, Ty) + G(Tx, x, Tz) + G(Ty, y, Tx) \\ & + G(Ty, y, Tz) + G(Tz, z, Tx) + G(Tz, z, Ty)], \end{aligned} \tag{5}$$

where $0 \leq \alpha, \beta, \gamma, \delta < 1$

$$0 \leq 2\beta + 4\gamma + 6\delta < 1, \tag{6}$$

$$0 \leq \alpha + 5\gamma + 5\delta < 1. \tag{7}$$

P r o o f. Consider a sequence $\{T^n x\}$ and let T is asymptotically regular at certain point $x_0 \in X$.

Assume that $u_n = T^n x_0$ and $u_m = T^m x_0$.

For $n, m \geq 1$

$$\begin{aligned}
&G(u_n, u_m, u_m)\\
&\leq \alpha G(u_{n-1}, u_{m-1}, u_{m-1}) + \beta[G(u_{n-1}, u_n, u_n) + 2G(u_{m-1}, u_m, u_m)]\\
&+ 2\gamma[G(u_{m-1}, u_n, u_n) + G(u_{n-1}, u_n, u_n) + G(u_{m-1}, u_m, u_m)]\\
&+ 2\delta[G(u_{n-1}, u_n, u_m) + G(u_{m-1}, u_m, u_n) + G(u_{m-1}, u_m, u_m)].
\end{aligned}$$

Now, using the rectangular inequality, we have

$$\begin{aligned}
&G(u_n, u_m, u_m)\\
&\leq \alpha[G(u_{n-1}, u_n, u_n) + G(u_{m-1}, u_m, u_m) + G(u_n, u_m, u_m)]\\
&+ \beta[G(u_{n-1}, u_n, u_n) + 2G(u_{m-1}, u_m, u_m)]\\
&+ 2\gamma[2G(u_{m-1}, u_m, u_m) + G(u_{n-1}u_n, u_n) + 2G(u_n, u_m, u_m)\\
&+ 2\delta[2G(u_{m-1}, u_m, u_m) + G(u_{n-1}u_n, u_n) + 2G(u_m, u_m, u_n)],
\end{aligned}$$

$$\begin{aligned}
G(u_n, u_m, u_m) \leq &\left\{\frac{(\alpha + \beta + 2\gamma + 2\delta)}{(1 - \alpha - 4\gamma - 4\delta)}\right\} G(u_{n-1}, u_n, u_n)\\
&+ \left\{\frac{(\alpha + 2\beta + 4\gamma + 4\delta)}{(1 - \alpha - 4\gamma - 4\delta)}\right\} G(u_{m-1}, u_m, u_m).
\end{aligned}$$

Taking limit as $n, m \to \infty$ on both sides, we have

$$\lim_{n,m\to\infty} G(u_n, u_m, u_m) = 0. \tag{8}$$

Since T is asymptotically regular mapping at certain point $x_0 \in X$,

$$G(u_{n-1}, u_n, u_n) \to 0 \text{ as } n \to \infty, \tag{9}$$

$$G(u_{m-1}, u_m, u_m) \to 0 \text{ as } m \to \infty. \tag{10}$$

To prove: $\{T^n x\}$ is Cauchy sequence

$$G(u_n, u_m, u_l) \leq G(u_n, u_m, u_m) + G(u_m, u_m, u_l).$$

Taking limit on both sides, we have

$$\lim_{n,m,l\to\infty} G(u_n, u_m, u_l) = 0. \tag{11}$$

So, $\{T^n x\}$ is Cauchy sequence.

Since (X, G) is a complete G-metric space, there exists $\mathrm{u} \in X$ such that

$$\mathrm{u} = \lim_{n\to\infty} u_n. \tag{12}$$

Suppose that $T\mathrm{u} \neq \mathrm{u}$,

$$\begin{aligned} G(\mathrm{u},&T\mathrm{u}, T\mathrm{u}) \\ &\leq G(\mathrm{u}, u_n, u_n) + G(u_{n-1}, T\mathrm{u}, T\mathrm{u}) \\ &\leq G(\mathrm{u}, u_n, u_n) + \alpha G(u_{n-1}, \mathrm{u}, \mathrm{u}) \\ &+ \beta[G(u_{n-1}, u_n, u_n) + 2G(\mathrm{u}, T\mathrm{u}, T\mathrm{u})] \\ &+ 2\gamma[G(\mathrm{u}, u_n, u_n) + G(u_{n-1}, T\mathrm{u}, T\mathrm{u}) + G(\mathrm{u}, T\mathrm{u}, T\mathrm{u})] \\ &+ 2\delta[G(u_{n-1}, u_n, T\mathrm{u}) + G(u_n, T\mathrm{u}, T\mathrm{u}) + G(\mathrm{u}, T\mathrm{u}, T\mathrm{u})]. \end{aligned}$$

Taking the limit as $n \to \infty$, we have

$$G(\mathrm{u}, T\mathrm{u}, T\mathrm{u}) < (2\beta + 4\gamma + 6\delta)G(\mathrm{u}, T\mathrm{u}, T\mathrm{u}). \tag{13}$$

This is contradiction.

Hence,

$$T\mathrm{u} = \mathrm{u}. \tag{14}$$

Suppose that T has a second fixed point v in X, then

$$\begin{aligned} G(\mathrm{u}, \mathrm{v}, \mathrm{v}) &= G(T\mathrm{u}, T\mathrm{v}, T\mathrm{v}) \\ &\leq \alpha G(\mathrm{u}, \mathrm{v}, \mathrm{v}) + \beta[G(\mathrm{u}, T\mathrm{u}, T\mathrm{u}) + 2G(\mathrm{v}, T\mathrm{v}, T\mathrm{v})] \\ &+ \gamma[2G(\mathrm{v}, T\mathrm{u}, T\mathrm{u}) + G(\mathrm{u}, T\mathrm{u}, T\mathrm{v}) + 2G(\mathrm{u}, T\mathrm{v}, T\mathrm{v})] \\ &+ \delta[G(\mathrm{u}, T\mathrm{u}, T\mathrm{v}) + 2G(\mathrm{u}, T\mathrm{v}, T\mathrm{v}) + 2G(\mathrm{v}, T\mathrm{u}, T\mathrm{u})], \\ G(\mathrm{u}, \mathrm{v}, \mathrm{v}) &< (\alpha + 5\gamma + 5\delta)G(\mathrm{u}, \mathrm{v}, \mathrm{v}). \end{aligned} \tag{15}$$

This contradiction implies that

$$\mathrm{u} = \mathrm{v}. \tag{16}$$

Thus, T has a unique fixed point. □

THEOREM 3.2. *In a complete symmetric G-metric space (X, G), a self mapping $T : X \to X$ has a unique fixed point and $\{T^n x\}$ also converging to a point in X if there exists an asymptotically regular mapping and $\{T^n x\}$ has a subsequence converging to a point in X, with for all $x, y, z \in X$, and condition* (5), (6) *and* (7) *hold.*

P r o o f. Consider a sequence $\{T^n x\}$ and let T is asymptotically regular at certain point $x_0 \in X$.

Assume that $u_n = T^n x_0$ and $u_{n_k} = T^{n_k} x_0$.

If

$$\lim_{k\to\infty} u_{n_k} = \mathrm{u}. \tag{17}$$

Suppose that $T\mathrm{u} \neq \mathrm{u}$,

$$\begin{aligned}
&G(\mathrm{u}, T\mathrm{u}, T\mathrm{u}) \\
&\quad \leq G(\mathrm{u}, u_{n_k}, u_{n_k}) + G(u_{n_k}, T\mathrm{u}, T\mathrm{u}) \\
&\quad \leq G(\mathrm{u}, u_{n_k}, u_{n_k}) + \alpha G(u_{n_k-1}, \mathrm{u}, \mathrm{u}) \\
&\quad + \beta[G(u_{n_k-1}, u_{n_k}, u_{n_k}) + 2G(\mathrm{u}, T\mathrm{u}, T\mathrm{u})] \\
&\quad + 2\gamma[G(\mathrm{u}, u_{n_k}, u_{n_k}) + G(u_{n_k-1}, T\mathrm{u}, T\mathrm{u}) + G(\mathrm{u}, T\mathrm{u}, T\mathrm{u})] \\
&\quad + 2\delta[G(u_{n_k-1}, u_{n_k}, T\mathrm{u}) + G(\mathrm{u}, T\mathrm{u}, u_{n_k}) + G(\mathrm{u}, T\mathrm{u}, T\mathrm{u})] \\
&\quad \leq G(\mathrm{u}, u_{n_k}, u_{n_k}) + \alpha G(u_{n_k-1}, \mathrm{u}, \mathrm{u}) + \beta[G(u_{n_k-1}, u_{n_k}, u_{n_k}) \\
&\quad + 2G(\mathrm{u}, T\mathrm{u}, T\mathrm{u})] + 2\gamma[G(\mathrm{u}, u_{n_k}, u_{n_k}) + G(u_{n_k-1}, u_{n_k}, u_{n_k}) \\
&\quad + G(u_{n_k-1}, T\mathrm{u}, T\mathrm{u}) + G(\mathrm{u}, T\mathrm{u}, T\mathrm{u})] + 2\delta[+G(\mathrm{u}, T\mathrm{u}, T\mathrm{u}) \\
&\quad + G(u_{n_k-1}, u_{n_k}, u_{n_k}) + G(u_{n_k}, u_{n_k}, T\mathrm{u}) + G(\mathrm{u}, T\mathrm{u}, u_{n_k})].
\end{aligned}$$

Taking the limit as $k \to \infty$, we obtain

$$G(\mathrm{u}, T\mathrm{u}, T\mathrm{u}) < (2\beta + 4\gamma + 4\delta)G(\mathrm{u}, T\mathrm{u}, T\mathrm{u}). \tag{18}$$

This contradiction implies that

$$T\mathrm{u} = \mathrm{u} \tag{19}$$

Hence, u is the fixed point of T.

By Theorem 3.1, we obtain u is the unique fixed point of T, using rectangular inequality in Def. 2.1.

Let us prove that: $\{T^n x\}$ converging to u in X.

$$\begin{aligned}
&G(\mathrm{u},u_n, u_n) \\
&\quad = G(T\mathrm{u}, u_n, u_n) \\
&\quad \leq \alpha G(\mathrm{u}, u_{n-1}, u_{n-1}) + \beta[G(\mathrm{u}, T\mathrm{u}, T\mathrm{u}) + 2G(u_{n-1}, u_n, u_n)] \\
&\quad + 2\gamma[G(u_{n-1}, T\mathrm{u}, T\mathrm{u}) + G(u_{n-1}, u_n, u_n) + G(\mathrm{u}, u_n, u_n)] \\
&\quad + 2\delta[G(\mathrm{u}, T\mathrm{u}, u_n) + G(u_{n-1}, u_n, T\mathrm{u}) + G(u_{n-1}, u_n, u_n)] \\
&\quad \leq \alpha[G(\mathrm{u}, u_n, u_n) + G(u_n, u_{n-1}, u_{n-1})] \\
&\quad + \beta[G(\mathrm{u}, T\mathrm{u}, T\mathrm{u}) + 2G(u_{n-1}, u_n, u_n)] \\
&\quad + 2\gamma[G(u_n, u_{n-1}, u_{n-1}) + 2G(T\mathrm{u}, u_n, u_n) + G(u_{n-1}, u_n, u_n)] \\
&\quad + 2\delta[G(u_{n-1}, u_n, u_n) + 2G(T\mathrm{u}, u_n, u_n) + G(u_{n-1}, u_n, u_n)],
\end{aligned}$$

$$\begin{aligned}
G(\mathrm{u}, u_n, u_n) \leq &\left\{ \frac{(2\beta + 2\gamma + 4\delta)}{(1 - \alpha - 4\gamma - 4\delta)} \right\} G(u_{n-1}, u_n, u_n) \\
&+ \left\{ \frac{(\alpha + 2\gamma}{(1 - \alpha - 4\gamma - 4\delta)} \right\} G(u_n, u_{n-1}, u_{n-1}).
\end{aligned}$$

As applying limit $n \to \infty$ on both sides and T is asymptotically regular, we obtain

$$\lim_{n\to\infty} G(\mathrm{u}, u_n, u_n) = 0. \tag{20}$$

Thus, $\{T^n x\}$ converging to u in X. □

4. **Digital image contraction algorithm**

Various partitioning strategies [16] are available in literature to improve in the image compression. In 2018, P. Bosilj et al. [13] is a comprehensive study on the hierarchical evolution of image representations in the recent past. Image data contraction requires removing non-essential information from an image, a process known as redundancy. There are three types of redundancies in an image: Redundancy in coding, psycho visual, and inter pixel. The limitations of the human visual system are used in conjunction with mismatching of image pixels, which is caused by similitude in nearby pixels, in the proposed method. Rectangular arrays of pixel values can be used to represent digital images. Any 8-bit grayscale digital image can be represented as an $m \times n$ matrix of pixel values, with each element indicating the pixel's grey value at the corresponding index. These pixels have 256 shades 0 to 255 in a greyscale of 8 bits, with 0 representing black and 255 representing white with 254 shades of grey in between.

The extend G-contraction condition (5) above Theorem 3.1 is as follows:

Where, $\alpha, \beta, \gamma, \delta$ contractivity factor, $0 \leq \alpha, \beta, \gamma, \delta < 1$.

Define a mapping $\mathcal{T} : \mathcal{A} \to \mathcal{A}$ given as:

$$\mathcal{T}(\mathcal{A}_i) = \max\{(\mathcal{A}_i) : (\mathcal{A}_i) \in \mathcal{A}\}. \tag{21}$$

$d =$ Matrix distance function is taken as Forbenius norm

$$d(A, B) = \sqrt{trace[(A - B)(A - B)']}. \tag{22}$$

As described in the following algorithm, the methodology involves parallel local operations on each element (pixel value) and immediate states.

The preceding steps are as follows:

(1) Upload image I in grayscale.
(2) As the pixel values of the input image, $A = [a_{i,j}], 1 \leq i \leq p,\ 1 \leq j \leq q$.
(3) Divide A into sub-matrices A_p^n using a fixed block of size $n \times n$ $(n \geq 2)$.
(4) Every sub-matrix A_p is processed to the extended G- contraction mapping T defined in (5), resulting in the contracted sub matrix B_p^1 of dimension $n \times n$. To get contracted matrix B, arrange each contracted sub matrix in the same order as the parent sub matrix.
(5) Obtain the reduced output image I'.

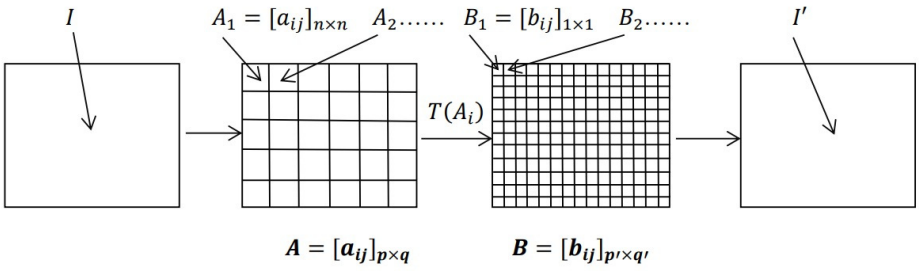

FIGURE 1. The above figure to show steps of scheme

5. **Proposed approach**

The proposed approach is implemented in Matlab. The algorithm takes the original images (I_1) in Fig. 2 and (I_2) in Fig. 3 as its input.

FIGURE 2. 512×512

FIGURE 3. 1024×1024

The intensity of each pixel of the input source images (I_1) in Fig. 2 is transformed to a subsequent $p \times q$ matrix A. Matrix A is then divided into $(n \geq 2)$ blocks (sub-matrices). Image segmentation is what this is all about. Each block is worked on separately, without regard for others, and can be processed concurrently if configured. Below are diagrams of the various stages involved. Consider a 16 pixel area of the original image (I_1) in Fig. 2. The first matrix belongs to the pixels of (I_1), which are divided into 64 non-overlapping blocks.

Each of them has a block size of 2×2 when treated to mapping (5), resulting in 64 non-overlapping blocks. $A_s^2, s = 1, 2, ..., 64$ each of size 1×1 are obtained, and from their sequential union matrix B with decreased dimension, picture (I_1') can be converted. The resulting contracted matrix is of varied size and values for the same input, $n > 2$.

For extending G-contraction condition from (5),

$$\begin{aligned} G(T(A_1),T(A2),T(A_3)) \leq \alpha[G(A_1,A_2,A_3)] \\ + \beta[G(T(A_1),A_1,T(A_1)) + G(T(A_2),A_2,T(A_2)) \\ + G(T(A_3),A_3,T(A_3))] + \gamma[G(T(A_1),A_2,T(A_1)) \\ + G(T(A_1),A_3,T(A_1)) + G(T(A_2),A_1,T(A_2)) \\ + G(T(A_2),A_3,T(A_2)) + G(T(A_3),A_1,T(A_3)) \\ + G(T(A_3),A_2,T(A_3))] + \delta[G(T(A_1),A_1,T(A_2)) \\ + G(T(A_1),A_1,T(A_3)) + G(T(A_2),A_2,T(A_1)) \\ + G(T(A_2),A_2,T(A_3)) + G(T(A_3),A_3,T(A_1)) \\ + G(T(A_3),A_3,T(A_2))]. \end{aligned} \tag{23}$$

Where, $\alpha, \beta, \gamma, \delta$ contractivity factor, $0 \leq \alpha, \beta, \gamma, \delta < 1$

$$0 \leq 2\beta + 4\gamma + 6\delta < 1, \tag{24}$$

$$0 \leq \alpha + 5\gamma + 5\delta < 1, \tag{25}$$

$$A = \begin{bmatrix} 127 & 123 & 125 & 120 & 126 & 123 & 127 & 128 & 125 & 129 & 129 & 132 \\ 128 & 126 & 128 & 122 & 125 & 125 & 122 & 129 & 127 & 128 & 131 & 128 \\ 128 & 124 & 128 & 126 & 127 & 120 & 128 & 129 & 128 & 131 & 135 & 126 \\ 124 & 127 & 128 & 129 & 121 & 128 & 129 & 128 & 129 & 133 & 130 & 132 \\ 126 & 125 & 128 & 126 & 126 & 125 & 127 & 128 & 131 & 127 & 128 & 136 \\ 125 & 127 & 126 & 126 & 128 & 128 & 128 & 126 & 130 & 129 & 128 & 131 \\ 127 & 127 & 128 & 124 & 120 & 127 & 128 & 126 & 128 & 131 & 134 & 127 \\ 123 & 135 & 120 & 128 & 121 & 123 & 126 & 126 & 128 & 133 & 131 & 129 \\ 126 & 128 & 124 & 128 & 125 & 123 & 128 & 130 & 128 & 132 & 128 & 131 \\ 124 & 128 & 127 & 124 & 127 & 121 & 128 & 130 & 132 & 133 & 133 & 128 \\ 122 & 126 & 128 & 126 & 123 & 127 & 124 & 129 & 131 & 134 & 130 & 130 \\ 126 & 127 & 125 & 122 & 125 & 121 & 127 & 128 & 131 & 131 & 132 & 129 \end{bmatrix},$$

$$T(A) = \begin{bmatrix} 128 & 128 & 126 & 129 & 129 & 132 \\ 128 & 129 & 128 & 129 & 133 & 135 \\ 127 & 128 & 128 & 128 & 131 & 136 \\ 135 & 128 & 127 & 128 & 133 & 134 \\ 128 & 128 & 127 & 130 & 133 & 133 \\ 127 & 128 & 127 & 129 & 134 & 132 \end{bmatrix}.$$

Let (A, G) be a $G-$metric space and define $G : A \times A \times A \to A$ by

$$G(A_1, A_2, A_3) = d(A_1, A_2) + d(A_2, A_3) + d(A_3, A_1), \tag{26}$$

where

$$d(A, B) = \sqrt{trace[(A - B)(A - B)']}. \tag{27}$$

Let $A_1 = \begin{bmatrix} 127 & 123 \\ 128 & 126 \end{bmatrix}$, $A_2 = \begin{bmatrix} 125 & 120 \\ 128 & 122 \end{bmatrix}$, and $A_3 = \begin{bmatrix} 126 & 123 \\ 125 & 125 \end{bmatrix}$,

$T(A_1) = [128]$, $T(A_2) = [128]$ and $T(A_3) = [126]$,

$$G(T(A)_1), T(A)_2), T(A)_3)) = 5 \tag{28}$$

$$G(A_1, A_2, A_3) = 13.9933 \tag{29}$$

$$G(T(A)_1), A_1, T(A)_1)) = 99.0152 \tag{30}$$

$$G(T(A)_2), A_2, T(A)_2)) = 0 \tag{31}$$

$$G(T(A)_3), A_3, T(A)_3)) = 4.4722 \tag{32}$$

$$G(T(A)_1), A_2, T(A)_1)) = 100 \tag{33}$$

$$G(T(A)_1), A_3, T(A)_1)) = 111.0496 \tag{34}$$

$$G(T(A)_2), A_1, T(A)_2)) = 2 \tag{35}$$

$$G(T(A)_2), A_3, T(A)_2)) = 11.4892 \tag{36}$$

$$G(T(A)_3), A_1, T(A)_3)) = 9.1652 \tag{37}$$

$$G(T(A)_3), A_2, T(A)_3)) = 8 \tag{38}$$

$$G(T(A)_1), A_1, T(A)_2)) = 51.5076 \tag{39}$$

$$G(T(A)_1), A_1, T(A)_3)) = 57.0902 \tag{40}$$

$$G(T(A)_2), A_2, T(A)_1)) = 51 \tag{41}$$

$$G(T(A)_2), A_2, T(A)_3)) = 6 \tag{42}$$

$$G(T(A)_3), A_3, T(A)_1)) = 60.7609 \tag{43}$$

$$G(T(A)_3), A_3, T(A)_2)) = 9.9807. \tag{44}$$

Substituting (28)-(44) in (23), we have

$$5 \leq \alpha(13.2253) + \beta(103.4874) + \gamma(241.7040) + \delta(236.3394). \tag{45}$$

For some $\alpha, \beta, \gamma, \delta \in [0, 1)$ in (45) satisfies the contractivity condition (24) and (25).

6. Results and analysis

6.1. Low Resolution Image (512 × 512).

The image (I_1) in Fig. 2 is utilized as an input to the method, and Figs. 4,5,6 and 7 shows that contracted images with decreased dimensions created using $n = 2, 3, 4$ and 5 as the fixed block size of the sub matrix, respectively.

FIGURE 4.

FIGURE 5.

FIGURE 6.

7.

FIGURE 8. Image reconstructed to original size after size reduction with 2 × 2 fixed size blocks, PSNR=26.67

FIGURE 9. Image reconstructed to original size after size reduction with 3 × 3 fixed size blocks, PSNR=21.27

FIGURE 10. Image reconstructed to original size after size reduction with 4×4 fixed size blocks,
PSNR=19.75

FIGURE 11. Image reconstructed to original size after size reduction with 5×5 fixed size blocks,
PSNR=18.00

The histogram shows Figs. 12, 13, 14 and 15 varying intensity values of the image in pixel. On 2×2 fixed block size of sub matrix the intensity level of the compressed image is reduced compared to the original image. The quality of image is not lost in the compressed image. On reconstruction the pixel intensity increasing back to the original intensity level which shown as Histogram in Fig. 12. In the same way image compresions are performed on the fixed block size of the submatrix 3×3, 4×4 and 5×5 respectively. Then, the pixel intensity reduces more on compression. On reconstructing, the original intensity is regained which is shown as Histogram in Figs. 13, 14 and 15. One of the most extensively utilized objective quality measures is PSNR [26]. Then the contracted image is retained to the dimension of the original image on reconstruction.

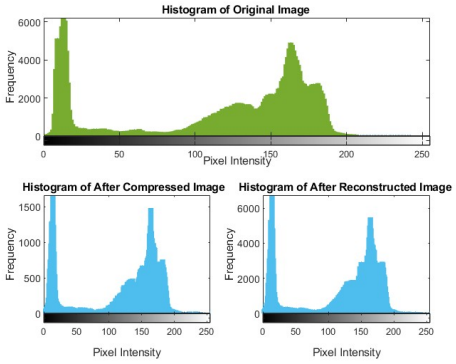

FIGURE 12. This Figure Shows Histogram of Figures 2, 4 and 8.

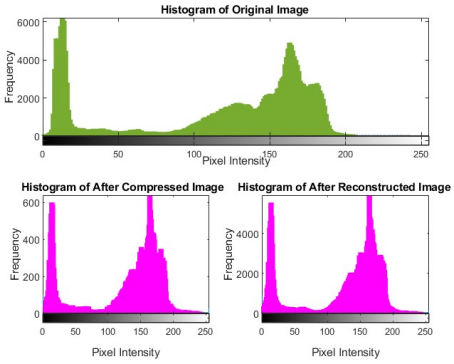

FIGURE 13. This Figure Shows Histogram of Figures 2, 5 and 9.

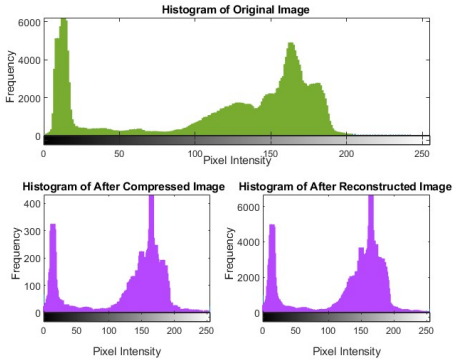

FIGURE 14. This Figure Shows Histogram of Figures 2, 6 and 10.

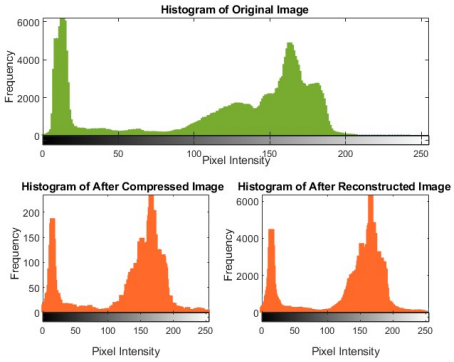

FIGURE 15. This Figure Shows Histogram of Figures 2, 7 and 11.

Table 1 and 2 summarizes the characteristics of contracted and reconstructed images. With image (I_1) as a reference in Fig. 2, the space saved can be computed, and the preset feature can be used repeatedly to reduce the image size even further. The 128×128 size in Fig. 10 can be attained either by contemplating dividing with a block size of 4×4 or by applying the scheme twice (iteratively) with a block size of 2×2 in each phase. The contracted

image will be nearly the same in both scenarios. The quality of a digital image that has been processed can be judged both subjectively and objectively.

TABLE 1. Summary of Original Image (I_1) After Contraced

	Test Image (I_1)	**Contracted**			
Figure	2	4	5	6	7
Dimension	512 × 512	256 × 256	170 × 170	128 × 128	102 × 102
Size (KB)	256	9.75	5.59	3.45	2.58
Block Size	-	2 × 2	3 × 3	4 × 4	5 × 5
% Space Saved	-	96.19	97.82	98.65	98.99

TABLE 2. Summary of Original Image (I_1) After Reconstructed

	Test Image (I_1)	**Reconstructed**			
Figure	2	8	9	10	11
Dimension	512 × 512	512 × 512	512 × 512	512 × 512	512 × 512
Size (KB)	256	25.2	28.1	23.6	27.7
Block Size	-	2 × 2	3 × 3	4 × 4	5 × 5
% Space Saved	-	90.15	89.02	90.78	89.18
PSNR	-	26.67	21.27	19.75	18.00

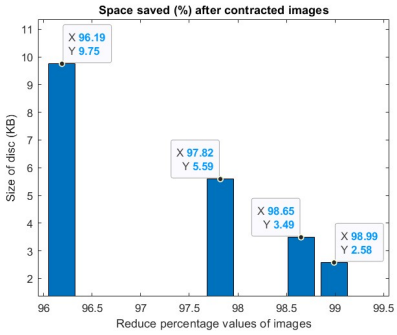

FIGURE 16. Bar graph shows contracted of images percentage values (I_1)

FIGURE 17. Bar graph shows reconstructed of images percentage values (I_1)

6.2. **High Resolution Image (1024 × 1024).**

The original image (I_2) in Fig. 3 is utilized as an input to the method, and Figs. 18,19,20 and 21 shows that contracted images with decreased dimensions created using $n = 2, 3, 4$ and 5 as the fixed block size of the sub matrix, respectively.

FIGURE 18.

FIGURE 19.

FIGURE 20.

21.

FIGURE 22. Image reconstructed to original size after size reduction with 2×2 fixed size blocks, PSNR=33.2001

FIGURE 23. Image reconstructed to original size after size reduction with 3×3 fixed size blocks, PSNR=29.8243

FIGURE 24. Image reconstructed to original size after size reduction with 4×4 fixed size blocks, PSNR=28.0885

FIGURE 25. Image reconstructed to original size after size reduction with 5×5 fixed size blocks, PSNR=26.1543

The histogram shows in Figs. 26, 27, 28 and 29 varying intensity values of the image in pixel. On 2×2 fixed block size of sub matrix the intensity level of the compressed image is reduced compared to the original image. The quality of image is not lost in the compressed image. On reconstruction the pixel intensity increases back to the original intensity level which shown as Histogram in Fig. 26. In the same way image compresions are performed on the fixed block size of the submatrix 3×3, 4×4 and 5×5 respectively. Then, the pixel intensity reduces more on compression. On reconstructing, the original intensity is regained which is shown as Histogram in Figs. 27, 28 and 29.One of the most extensively utilized objective quality measures is PSNR [26]. Then the contracted image is retained to the dimension of the original image on reconstruction.

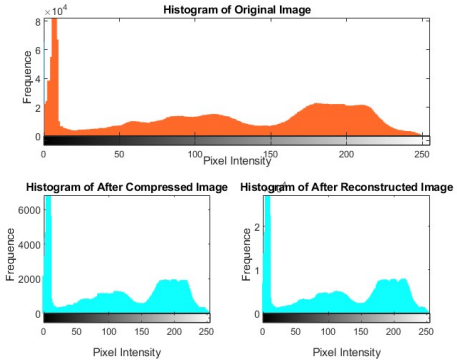

FIGURE 26. This Figure Shows Histogram of Figures 3, 18 and 22.

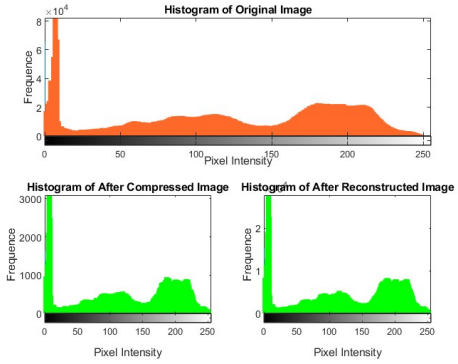

FIGURE 27. This Figure Shows Histogram of Figures 3, 19 and 23.

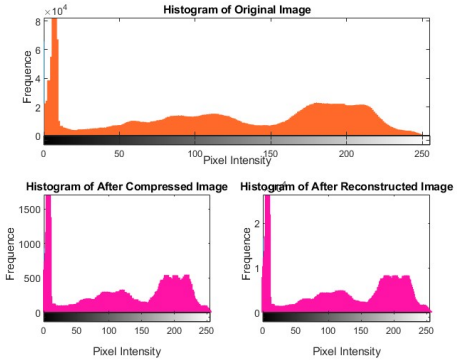

FIGURE 28. This Figure Shows Histogram of Figures 3, 20 and 24.

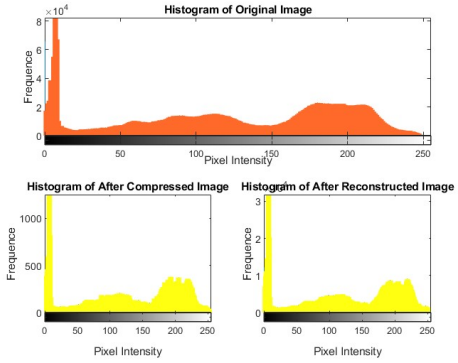

FIGURE 29. This Figure Shows Histogram of Figures 3, 21 and 25.

Table 3 and 4 summarizes the characteristics of contracted and reconstructed images. With original image in Fig. 3 as a reference, the space saved can be computed, and the preset feature can be used repeatedly to reduce the image size even further. The 256×256 size in Fig. 20 can be attained either by contemplating dividing with a block size of 4×4 or by applying the scheme twice (iteratively) with a block size of 2×2 in each phase. The contracted

image will be nearly the same in both scenarios. The quality of a digital image that has been processed can be judged both subjectively and objectively.

TABLE 3. Summary of Original Image (I_2) After Contracted

	Test Image (I_2)	**Contracted**			
Figure	3	18	19	20	21
Dimension	1024 × 1024	512 × 512	341 × 341	256 × 256	204 × 204
Size (KB)	98.2	26.4	12.6	7.85	5.56
Block Size	-	2 × 2	3 × 3	4 × 4	5 × 5
% Space Saved	-	73.12	87.17	92.00	94.37

TABLE 4. Summary of Original Image (I_2) After Reconstructed

	Test Image (I_2)	**Reconstructed**			
Figure	3	22	23	24	25
Dimension	1024 × 1024	1024 × 1024	1024 × 1024	1024 × 1024	1024 × 1024
Size (KB)	98.2	63.8	62.4	53.8	63.1
Block Size	-	2 × 2	3 × 3	4 × 4	5 × 5
% Space Saved	-	35.03	36.45	45.21	35.74
PSNR	-	33.2001	29.8243	28.0885	26.1543

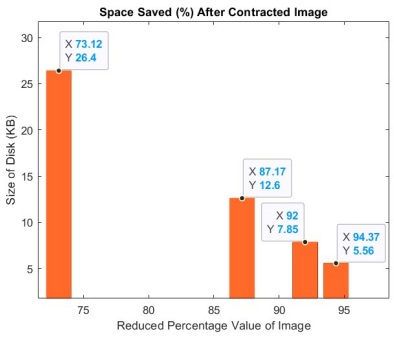

FIGURE 30. Bar graph shows contracted of images percentage values (I_2)

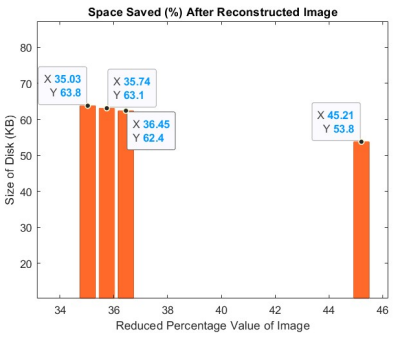

FIGURE 31. Bar graph shows reconstructed of images percentage values (I_2)

7. Conclusion

For image processing, the metric is formulated suitably on a continuous digital space, which is subsequently discretized as pixels. Extended G-contraction mapping on function maximum has been defined and applied to obtain contracted images. It is important to note that the original image size decreased without losing quality. As a result, the contracted image obtained has a smaller size and requires less storage space, making it easier to send. The technique is tested on various block sizes to see how far an image can be compressed. The developed function is iterated repeatedly on the input image, the resulting final contracted image is of high quality if the input image is enlarge and has low color fluctuation. Also, the contracted to the dimension of the original image size with moderate image pixel quality. PSNR value is used to calculate the difference between the quality of the original and the renovated image.

References

[1] S. Banach, Sur les operations dans les ensembles abstraits et leurs applications aux equations integrales, *Fund. Math.*, **3** (1922), 133-181.

[2] S. Gahler, 2-Metrices Raume und Ihre Topologische Struktur, *Mathematische Nachrichten*, **26** (1963), 115-148.

[3] B. C. Dhage, Generalized Metric Spaces and Mappings with Fixed Point, *Bulletin of Calcutta Mathematical Society*, **84** (1992), 329-336.

[4] Z. Mustafa, B. Sims, Some remarks concerninig d-metric spaces, *Proceeding of the International Conferences on Fixed Point Theory and Applications*, (2003), 189-198.

[5] Z. Mustafa, B. Sims, A new approach to generalized metric spaces, *Journal of Nonlinear and Convex Analysis*, **7** (2006), 287-297.

[6] A. Azam, B. Fisher, M. Khan, Common fixed point theorems in complex valued metric spaces, *Numer. Funct. Anal. Optim.*, **33** (2011), 243-253.

[7] L. Boxer, Digitally continuous functions, *Pattern Recognit. Lett.*, **15** (1994), 833-839.

[8] F. E. Browder and W. V. Petryshyn, The solution by iteration of non linear functional equations in Banach spaces, *Bull. Amer. Math. Soc.*, **72** (1966), 571–575.

[9] O. Ege, I. Karaca, Fundamental properties of simplicial homology groups for digital images, *American Journal of Computer Technology and Application*, **1** (2013), 25-42.

[10] O. Ege, I. Karaca, Banach fixed point theorem for digital images, *J. Nonlinear Sci. Appl.*, **8** (2015), 237-245.

[11] R. Anna Thirumalai, S. Thalapathiraj, A novel approach for digital image compression in some fixed point results on complete G-metric space using comparison function, *Int. J. Anal. Appl.*, **21** (2023), 110.

[12] S. Thalapathiraj, B. Baskaran, J. Arunnehru, A block based secret sharing scheme using Hilbert matrix and RSA, *AIP Conference Proceedings*, **2112** (2019).
[13] P. Bosilj, E. Kijak, S. Lefèvre, Partition and inclusion hierarchies of images: a comprehensive survey, *J. Imaging.*, **33** (2018).
[14] S. E. Han, Banach fixed point theorem from the viewpoint of digital topology, *J. Nonlinear Sci. Appl.*, **9** (2016), 895-905.
[15] S. E. Han, Connected sum of digital closed surfaces, *Inform. Sci.*, **176** (2006), 332-348.
[16] L. G. Huang, X. Zhang, Cone metric spaces and fixed point theorems of contractive mappings, *J. Math. Anal. App.*, **332** (2007), 1468-1476.
[17] M. Jleli, B. Samet, Remarks on g-metric spaces and fixed point theorems, *Fixed Point Theory Appl.*, **2012** (2012).
[18] I. Karaca, O. Ege, Some results on simplicial homology groups of 2D digital images. *Int. J. Inform. Computer Sci.*, **1**(2012), 198-203.
[19] A. Rosenfeld, Digital topology, *Amer. Math. Mon.*, **86** (1979).
[20] G. Prasad, R. C. Dimri, Fixed point theorems via comparable mappings in ordered metric spaces, *J. Anal.*, **27** (2019), 1139-1150.
[21] Durdana Lateef, Fisher type fixed point results in controlled metric spaces, *J. Math. Computer Sci.*, **20** (2020), 234-240.
[22] R. Anna Thirumalai, S. Thalapathiraj, Solution of the boundary value problems via fixed point theorem on G-metric space, *IAENG International Journal of Applied Mathematics*, **53** (2023), 1357-1369.
[23] K Hemavathy, S. Thalapathiraj, Common Fixed Point Theorems for 2-Metric Space using Various EA Properties, *IAENG International Journal of Applied Mathematics*, **53** (2023), 1-7.
[24] R. Anna Thirumalai, S. Thalapathiraj, C. Rajesh, Some common fixed point results in complete G-metric space by using four mappings, *AIP Conf. Proc.*, **2852** (2023).
[25] A. El Haddouchi, B. Marzouki, A generalized fixed point theorem in G-metric space, *Journal of Analysis and Applications*, **17** (2019), 89-105.
[26] K. H. Thung, P. Raveendran, A survey of image quality measures, *International Conference for Technical Postgraduates (TECHPOS)*, (2009), 1-4.
[27] Samjhana Koirala, Narayan Prasad Pahari, Some results on fixed point theory in G-metric space, *International Journal of Mathematics Trends and Technology*, **67** (2021), 150-156.
[28] Narinder Kumar, Manoj Kumar, Ashish, Fixed point theory for simulation functions in G-metric spaces: A novel approach, *Advances in Fixed Point Theory*, *12* (2022), 9 pages.
[29] Budi Nurwahyu, Naimah Aris, Firman, Some results in function weighted b-metric spaces, *AIMS Mathematics*, **8** (2023), 8274-8293.

[30] Deepthi K. Oommen, J. Arunnehru, Alzheimer's disease stage classification using a deep transfer learning and sparse auto encoder method, *Computers, Materials and Continua*, **76** (2023), 793-811.

[31] Deepthi K. Oommen, J. Arunnehru, Detection and classification of Alzheimer's Disease: A deep learning approach with predictor variables, *Diagnosis of Neurological Disorders Based on Deep Learning Techniques*, (2023), 85-98.

[32] R. Rajkumar, J. Arunnehru, A study on convolutional neural networks with active video tubelets for object detection and classification, *Soft Computing and Signal Processing: Proceedings of ICSCSP 2018* (2019), 107-115.